STATISTICS, OPTIMIZATION AND INFORMATION COMPUTING
Stat., Optim. Inf. Comput., Vol. **15**, April 2026, pp 3341–3365.
Published online in International Academic Press (www.IAPress.org)

Exploring the Dynamics of Malaria in East Nusa Tenggara, Indonesia: Impact of Relapse, Treatment and Vaccination

Chidozie W. Chukwu [1,*], Josiah Mushanyu [2], Stephane Y. Tchoumi [3]

[1]*Department of Mathematical Sciences, Georgia Southern University, Statesboro, Georgia, 30460, USA*
[2]*Department of Computing, Mathematical & Statistical Science, University of Namibia, Windhoek 13301, Namibia*
[3]*Department of Mathematics and Computer Sciences ENSAI, University of Ngaoundere, Cameroon*

Abstract Malaria infection continues to affect numerous countries worldwide, persisting as a public health issue despite recent progress in control measures. Particularly in regions like Africa and the Middle East, malaria remains a significant concern. We formulate two mathematical models to evaluate how vaccination and treatment efforts contribute to combating malaria. Parameter estimation and model validation are performed using the dataset for malaria incidence from Lembata Regency, East Nusa Tenggara Province, Indonesia. The first model is motivated by the increasing demand for a malaria vaccine. Our study results suggest that such a vaccine could reduce the global prevalence of malaria. The second model includes two types of treatment: radical cure and bloodstream treatments. The model reproduction numbers and equilibrium points for both models are established. A global sensitivity analysis is conducted to identify the parameters that significantly impact the model's reproduction number. Numerical analysis is carried out to support theoretical findings. The extended model results give the necessary malaria control thresholds to lower the $\mathcal{R}_c^t$ value to fully eradicate malaria in Lembata Regency, East Nusa Tenggara Province, Indonesia. Both models demonstrate the vital importance of vaccination and treatment in combating malaria infection.

Keywords Malaria, Vaccination, Treatment, Sensitivity analysis, Numerical simulations

AMS 2010 subject classifications 34D05, 92D30

DOI: 10.19139/soic-2310-5070-3111

1. Introduction

Malaria, a parasitic disease spread by Anopheles mosquitoes, continues to pose a major global health risk, particularly in Africa, Southeast Asia, the eastern Mediterranean, and the Western Pacific [3]. According to the World Health Organization's Malaria 2020 Report, there were an estimated 228 million cases of malaria and 409,000 deaths worldwide in 2019, with Africa alone accounting for 94% of cases. Common symptoms of malaria include fever, chills, headache, muscle aches, fatigue, nausea, vomiting, and sometimes diarrhea [4]. Early diagnosis is crucial, followed by prompt treatment with appropriate antimalarial drugs to prevent the disease from becoming severe and life-threatening [4]. Indonesia, located in Southeast Asia, boasts a diverse population of around 265 million people, consisting of 1,340 ethnic groups scattered throughout the archipelago [22]. By 2018, 285 out of 514 districts, accounting for 55.5% of the nation's districts, had successfully eliminated malaria [8]. However, regions such as Papua, West Papua, Maluku, North Maluku, and East Nusa Tenggara Province (ENTP)

*Correspondence to: Chidozie W. Chukwu (Email: cchukwu@georgiasouthern.edu). Department of Mathematical Sciences, Georgia Southern University, Statesboro, Georgia, 30460, USA.

ISSN 2310-5070 (online) ISSN 2311-004X (print)

have not yet achieved this goal but aim to do so by 2030 [8]. A 2018 Annual Parasite Incidence (API) survey indicated a national API of 0.84 per 1000 people, with significant variations among the 34 provinces. Papua had the highest API at 52.99 per 1000 people, while the ENTP (the focus of the proposed study), had an API of 3.42 per 1000 people [22]. Despite a steady nationwide decline in API from 1.8 per 1000 in 2009 to 0.84 per 1000 in 2018, the ENTP's API remained above the national average. Although the ENTP's API decreased from 13.7 per 1000 people in 2014 to 3.42 per 1000 people in 2018, it still exceeded the national API level [18].

Therefore, modeling malaria transmission is crucial for evaluating the effectiveness of control measures in stemming the spread of malaria in the ENTP. This endeavor holds paramount importance in reducing the elevated rates of morbidity and mortality linked to malaria infections. Despite ongoing efforts to control and eradicate malaria-related mortality, the disease remains a global health concern, particularly in endemic regions like Africa and the Middle East [17, 5]. While there has been a decrease in malaria cases over recent decades, it still poses a threat to communities in certain areas. Recurrent phenomena such as relapse, reinfection, and recrudescence frequently occur in infected individuals, exacerbating the malaria burden [31, 35]. Relapse, primarily associated with P. vivax and ovale species, occurs when dormant parasites in the liver reactivate, leading to renewed malaria infection [35]. Malaria treatment involves using antimalarial drugs to eliminate the Plasmodium parasites from the human body. Treatment choice depends on factors such as the Plasmodium species causing the infection, the severity of symptoms, and the geographic location of the infected human. The summarized overview of malaria treatment involves using antimalarial drugs, preventive treatment (chemoprophylaxis), transmission-blocking, and many others. To date, global health organizations, including the WHO, are actively involved in controlling and eliminating malaria by distributing effective antimalarial drugs, preventive measures, and research on new treatment methodologies. Despite these efforts, malaria elimination in most WHO-classified endemic regions has yet to be achieved. Some of these efforts include developing a more general vaccine for all age groups, not just the malaria vaccine for children, RTS, S/AS01 (Mosquirix). Other malaria control methods include using a mosquito-bed net, vector control, surveillance and monitoring, early diagnosis and treatment, and so on [23].

Several mathematical models have been formulated to study malaria transmission dynamics and the effects of several interventions and control measures to help mitigate malaria infection. Tasman *et al.* [35] investigated the impact of relapse, reinfection, and recrudescence on malaria eradication policy. On the other hand, Handari *et al.* [23] proposed an $SEIRS$ malaria model to study the potential impact of the new malaria pre-erythrocytic vaccine and transmission-blocking treatment and found that both the pre-erythrocytic vaccine and transmission-blocking treatment significantly reduce the spread of malaria in Papua and West Papua, Indonesia. Recent work from East Nusa Tenggara Province highlights that malaria transmission in the region remains closely tied to behavioral, socioeconomic, and access-related factors. In a cross-sectional study conducted across high-, moderate-, and low-endemic settings in rural ENTP, Guntur *et al.* [40] found generally low levels of malaria awareness, with pronounced differences in knowledge, prevention practices, and treatment-seeking behavior between communities. Their results suggest that limited awareness and delayed care-seeking continue to hinder effective malaria control, particularly in areas with higher endemicity. Using longitudinal health-facility data, Lobo *et al.* [41] examined malaria trends in rural ENTP over ten years and reported an overall decline in malaria prevalence. However, this decline was not uniform over time; the authors observed periods of resurgence, including an increase in *Plasmodium falciparum* cases during the COVID-19 period, indicating that progress toward elimination in the province remains fragile and vulnerable to disruptions in healthcare delivery. Further, Guntur *et al.* [42] investigated malaria risk factors among adults living in hilly and hard-to-reach communities in ENTP. Their analysis showed that a history of malaria was strongly associated with low educational attainment, poor malaria knowledge, inconsistent bed-net use, and outdoor occupational exposure. Taken together, these ENTP-specific studies emphasize that malaria persistence in the province is driven not only by biological factors but also by human behavior and uneven access to prevention and treatment services, underscoring the importance of locally tailored control strategies. The interested reader is referred to the following published literature where several models have been formulated and analyzed to investigate reinfection [27, 21], mosquito seasonality [34, 24], use of bed net [9], optimal control [28], relapse [10], treatment [25] and vaccinations [38] concerning the transmission

path of malaria with lucrative suggestion on possible control strategies to control/eradicate malaria across different regions of the globe.

In 2021, WHO developed a malaria 2016–2030 strategy to reduce malaria case incidence and mortality rates by at least 30%, thereby eliminating malaria in at least 35 endemic regions by the year 2030 [6]. Importantly, preventing a resurgence of malaria in all malaria-free countries through regional/country guidance and support programs towards malaria control and elimination. Following the literature review presented in the above mathematical models and the WHO goal for malaria elimination, we formulate a new malaria model to investigate the potential impact of vaccination, relapse, and treatment on the spread of malaria with a specific application to the dataset for malaria incidence data from Lembata Regency, ENTP, Indonesia. Due to the high incidence of malaria in this province of Indonesia, we sought to study the potential impact of the malaria dynamics with the available historical data to help predict the optimal control or combined strategy required to curb the spread of malaria in ENTP Indonesia.

Although Indonesia has made substantial progress toward malaria elimination, ENTP continues to experience persistent transmission, driven by relapse-prone infections, heterogeneous treatment access, and geographic barriers to healthcare delivery. Existing studies on ENTP primarily focus on epidemiological trends, awareness, and risk factors; however, there is a lack of mechanistic transmission models calibrated to local data that explicitly account for relapse and treatment pathways. This gap limits the ability to assess intervention thresholds and combined control strategies in this setting. Motivated by this need, this study makes three main contributions. First, we develop a deterministic malaria transmission model that incorporates relapse dynamics, along with vaccination, to explore their combined effects in a relapse-prone environment. Second, we extend the framework to include two treatment pathways: bloodstream treatment and radical cure, reflecting key clinical aspects of malaria management in ENTP. Third, we calibrate the vaccination model using incidence data from Lembata Regency and quantify parameter uncertainty through bootstrap-based confidence intervals. Together, these contributions provide a tractable, data-informed modeling framework for evaluating malaria control strategies in ENTP and similar resource-limited settings. The next section presents the formulation of the deterministic model, followed by its mathematical analysis.

Table 1. Parameter description of the model with vaccination.

Symbols	Definitions
Λ_h	Human recruitment rate
Λ_v	Mosquitoes recruitment rate
b	Contact rate between mosquitoes and humans
p_m	Transmission probability from human to mosquitoes
p_h	Transmission probability from mosquitoes to human
μ_d	Disease-induced mortality rate
μ_h	Human death rate
ψ	Relapse rate
μ_v	Mosquito death rate
γ	Human recovery rate
ω	Rate of loss of vaccination immunity
τ	Rate of progression from exposed to infectious humans
δ	Rate of progression from latent to susceptible humans
v_1	Vaccination rate for susceptible humans
v_2	Vaccination rate for humans in the latency stage
κ	Rate of progression from exposed to infectious mosquitoes
α	Probability of perfect and definitive protection by vaccine
ε	Proportion of symptomatic infected individuals progressing to L_h

2. The mathematical model with vaccination

We formulate a mathematical model that incorporates malaria vaccination as a control mechanism. The model divides the total population into distinct compartments based on the disease status. The human population comprises susceptible (S_h), exposed (E_h), symptomatic infected (I_h), latently infected (L_h), and vaccinated (V) individuals. Note that individuals in the latent class L_h are considered to be asymptomatic individuals who still harbor the malaria-causing parasites in their liver after recovering from malaria. This is consistent with the clinical observations on malaria, where the parasites responsible for the disease, such as Plasmodium spp., can persist in the liver in a dormant or latent form. However, after some time, the reservoir of malaria parasites in the liver can deteriorate an individual's health, leading to a relapse of the infection. It is worth noting that the specific details of the latent phase can vary depending on the Plasmodium species causing the infection (e.g., Plasmodium vivax is known for its ability to form dormant liver stages). The model also tracks malaria transmission in the mosquito population. We subdivide the mosquito population into three distinct compartments, namely, susceptible (S_v), exposed (E_v), and infected (I_v) mosquitoes. The model considers administering vaccination to susceptible humans and those who are latently infected. Parameter descriptions are summarized in Table 1 while Figure 1 shows the possible interactions between human and mosquito populations in the context of malaria infection.

Combining the schematic diagram (Figure 1), the model parameters, and state variables descriptions given above lead to the following non-linear ordinary differential equations:

$$\begin{cases} \dfrac{dS_h}{dt} = \Lambda_h - \dfrac{bp_h S_h I_v}{N_h} + \delta L_h + (1-\epsilon)\gamma I_h + (1-\alpha)\omega V_h - (\mu_h + v_1)S_h, \\ \dfrac{dE_h}{dt} = \dfrac{bp_h(S_h + L_h)I_v}{N_h} - (\mu_h + \tau)E_h, \\ \dfrac{dI_h}{dt} = \tau E_h + \psi L_h - (\mu_h + \mu_d + \gamma)I_h, \\ \dfrac{dL_h}{dt} = \varepsilon\gamma I_h - \dfrac{bp_h L_h I_v}{N_h} - (\mu_h + \delta + \psi + v_2)L_h, \\ \dfrac{dV_h}{dt} = v_1 S_h + v_2 L_h - (1-\alpha)\omega V_h - \mu_h V_h, \\ \dfrac{dS_v}{dt} = \Lambda_v - \dfrac{bp_m S_v I_h}{N_h} - \mu_v S_v, \\ \dfrac{dE_v}{dt} = \dfrac{bp_m S_v I_h}{N_h} - (\mu_v + \kappa)E_v, \\ \dfrac{dI_v}{dt} = \kappa E_v - \mu_v I_v, \end{cases} \tag{1}$$

with initial conditions

$$S_h(0) > 0,\ E_h(0) \geq 0,\ I_h(0) \geq 0,\ L_h(0) \geq 0,\ V_h(0) \geq 0,\ S_v(0) > 0,\ E_v(0) \geq 0,\ I_v(0) \geq 0$$

where all the model parameters are assumed to be positive.

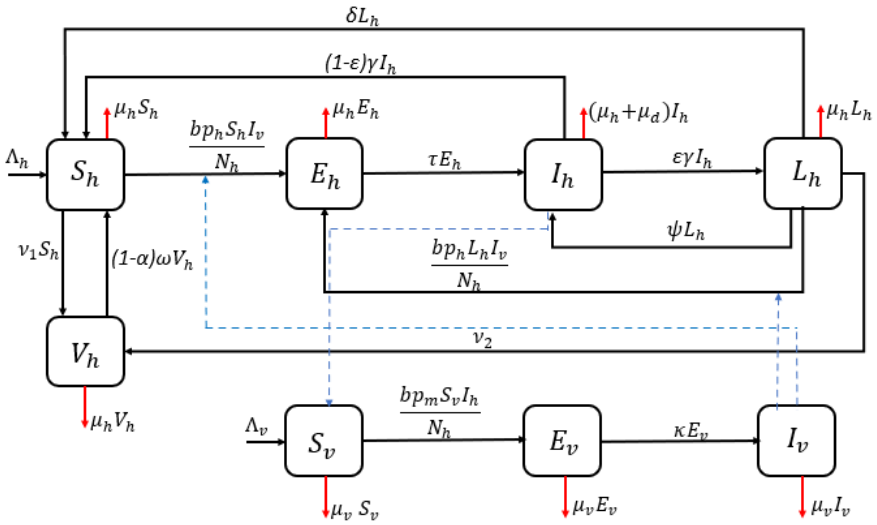

Figure 1. Model flow diagram.

2.1. Fundamental properties

It can be easily demonstrated that system (1) has positive solutions $\forall t > 0$. This is stated in the following theorem (Theorem 1). The proof can be carried out similarly as in [26, 14].

Theorem 1
For non-negative initial condition $S_h(0) \geq 0, E_h(0) \geq 0, I_h(0) \geq 0, L_h(0) \geq 0,$
$V_h(0) \geq 0, S_v(0) \geq 0, E_v(0) \geq 0, I_v(0) \geq 0,$ there exists $(S_h(t), E_h(t), I_h(t), L_h(t), V_h(t), S_v(t), E_v(t), I_v(t)) : (0, \infty) \to (0, \infty)$ which solve system (1).

We now study system (1) in the following biologically feasible region:

$$\Omega = \left\{ (S_h, E_h, I_h, L_h, V_h) \in \mathbb{R}^5_+ \mid N_h \leq \frac{\Lambda_h}{\mu_h},\ (S_v, E_v, I_v) \in \mathbb{R}^3_+ \mid N_v \leq \frac{\Lambda_v}{\mu_v} \right\}. \tag{2}$$

In order to ensure that Model (1) is well posed, such that all solutions with initial conditions start and remain in Ω-region for all time $t > 0$, we state the following theorem.

Theorem 2
The compact region Ω defined in (2) is positively invariant with respect to the system (1) and attracts all solutions in $\mathbb{R}^8_+$.

Proof
Let $\mathcal{N}(t) = (N_h(t), N_v(t)) = (S_h(t) + E_h(t) + I_h(t) + L_h(t) + V_h(t), S_v(t) + E_v(t) + I_v(t))$. The time derivative of $\mathcal{N}(t)$ is given by

$$\frac{d\mathcal{N}}{dt} = \left(\frac{dN_h}{dt}, \frac{dN_v}{dt} \right) = \left(\frac{dS_h}{dt} + \frac{dV_h}{dt} + \frac{dE_h}{dt} + \frac{dI_h}{dt} + \frac{dL_h}{dt}, \frac{dS_v}{dt} + \frac{dE_v}{dt} + \frac{dI_v}{dt} \right)$$

where

$$\begin{cases} \dfrac{dN_h}{dt} & = \Lambda_h - \mu_d I_h - \mu_h \left(S_h + E_h + V_h + I_h + L_h \right) \leq \Lambda_h - \mu_h N_h \leq 0, \text{ for } N_h \geq \dfrac{\Lambda_h}{\mu_h} \\ \dfrac{dN_v}{dt} & = \Lambda_v - \mu_v \left(S_v + E_v + I_v \right) = \Lambda_v - \mu_v N_v \leq 0, \text{ for } N_v \geq \dfrac{\Lambda_v}{\mu_v}. \end{cases} \tag{3}$$

whose solutions yield

$$\begin{cases} N_h(t) & \leq \dfrac{\Lambda_h}{\mu_h} + \left(\dfrac{\Lambda_h}{\mu_h} + N_h(0)\right) e^{-\mu_h t} \\ N_v(t) & \leq \dfrac{\Lambda_v}{\mu_v} + \left(\dfrac{\Lambda_v}{\mu_v} + N_v(0)\right) e^{-\mu_v t}. \end{cases} \tag{4}$$

Thus, $\dfrac{d\mathcal{N}}{dt} \leq 0$ from (3), which implies that Ω is a positively invariant set. Also, from (4) we obtain

$$0 \leq (N_h(t), N_v(t)) \leq \left(\frac{\Lambda_h}{\mu_h} + \left(\frac{\Lambda_h}{\mu_h} + N_h(0)\right) e^{-\mu_h t}, \ \frac{\Lambda_v}{\mu_v} + \left(\frac{\Lambda_v}{\mu_v} + N_v(0)\right) e^{-\mu_v t}\right).$$

Thus, $0 \leq (N_h(t), N_v(t)) \leq \left(\dfrac{\Lambda_h}{\mu_h}, \dfrac{\Lambda_v}{\mu_v}\right)$ as $t \to \infty$ and hence Ω is an attractive set. Therefore, if the vector field of system (1) is restricted to the boundary of Ω, then it will not contain an exterior point of Ω. This means all solutions with initial conditions starting in Ω will remain in Ω for all time $t > 0$. □

2.2. Disease-free equilibrium and the control reproduction number of system (1)

We first establish the disease-free equilibrium (DFE), a state depicting the absence of malaria disease. The DFE for Model (1) is calculated to be

$$\mathcal{E}_0 = (S_h^o, E_h^o, I_h^o, L_h^o, V_h^o, S_v^o, E_v^o, I_v^o) = \left(\frac{((1-\alpha)\omega + \mu_h)\Lambda_h}{((1-\alpha)\omega + \mu_h + v_1)\mu_h}, 0, 0, 0, \frac{\Lambda_h v_1}{\mu_h((1-\alpha)\omega + \mu_h + v_1)}, \frac{\Lambda_v}{\mu_v}, 0, 0\right).$$

To derive the control reproduction number for Model (1), we follow the next-generation matrix approach outlined in van den Driessche [37]. Let $\boldsymbol{x} = (E_h, I_h, L_h, E_v, I_v)$. We define the vector $\mathcal{F}(\boldsymbol{x})$ whose i-th entry represent the rate of new infections in the i-th entry of the vector $\boldsymbol{x}$ and $\mathcal{V}(\boldsymbol{x})$ whose i-th entry represent the transition rate out of the i-th entry of the vector $\boldsymbol{x}$. Then, we can find

$$\mathcal{F}(\boldsymbol{x}) = \begin{pmatrix} \frac{bp_h(S_h+L_h)I_v}{N_h} \\ 0 \\ 0 \\ \frac{bp_m S_v I_h}{N_h} \\ 0 \end{pmatrix} \quad \mathcal{V}(\boldsymbol{x}) = \begin{pmatrix} a_1 E_h \\ -\tau E_h + a_2 E_h - \psi L_h \\ -\epsilon\gamma I_h + a_3 L_h \\ a_4 E_v \\ -\kappa E_v + \mu_v I_v \end{pmatrix} \tag{5}$$

where $a_1 = \mu_h + \tau$, $a_2 = \gamma + \mu_d + \mu_h$, $a_3 = \delta + \mu_h + \nu_2 + \psi$, $a_4 = \kappa + \mu_v$. We then find the matrix to represent the new infections and the transition between compartments by determining the Jacobian of $\mathcal{F}(\boldsymbol{x})$ and $\mathcal{V}(\boldsymbol{x})$ evaluated at $\mathcal{E}_0$. Let F and V be the respective Jacobian matrices of $\mathcal{F}(\boldsymbol{x})$ and $\mathcal{V}(\boldsymbol{x})$ evaluated at DFE,

$$F = \begin{pmatrix} 0 & 0 & 0 & 0 & \frac{bp_h((1-\alpha)\omega+\mu_h)}{(1-\alpha)\omega+\mu_h+\nu_1} \\ 0 & 0 & 0 & 0 & 0 \\ 0 & 0 & 0 & 0 & 0 \\ 0 & \frac{b\mu_h p_m \Lambda_v}{\Lambda_h \mu_v} & 0 & 0 & 0 \\ 0 & 0 & 0 & 0 & 0 \end{pmatrix} \quad \text{and} \quad V = \begin{pmatrix} a_1 & 0 & 0 & 0 & 0 \\ -\tau & a_2 & -\psi & 0 & 0 \\ 0 & -\gamma\epsilon & a_3 & 0 & 0 \\ 0 & 0 & 0 & a_4 & 0 \\ 0 & 0 & 0 & -\kappa & \mu_v \end{pmatrix}.$$

We then obtain

$$FV^{-1} = \begin{pmatrix} 0 & 0 & 0 & F_{14} & F_{15} \\ 0 & 0 & 0 & 0 & 0 \\ 0 & 0 & 0 & 0 & 0 \\ F_{41} & F_{42} & F_{43} & 0 & 0 \\ 0 & 0 & 0 & 0 & 0 \end{pmatrix}$$

where

$$F_{14} = \frac{b\kappa p_h\left((1-\alpha)\omega+\mu_h\right)}{a_4\mu_v\left((1-\alpha)\omega+\mu_h+\nu_1\right)}, \qquad F_{15} = \frac{bp_h\left((1-\alpha)\omega+\mu_h\right)}{\mu_v\left((1-\alpha)\omega+\mu_h+\nu_1\right)},$$

$$F_{41} = \frac{a_3b\tau\mu_h p_m\Lambda_v}{a_1a_2a_3\Lambda_h\mu_v - a_1\gamma\psi\epsilon\Lambda_h\mu_v}, \qquad F_{42} = \frac{a_3b\mu_h p_m\Lambda_v}{a_2a_3\Lambda_h\mu_v - \gamma\psi\epsilon\Lambda_h\mu_v},$$

$$F_{43} = \frac{b\psi\mu_h p_m\Lambda_v}{a_2a_3\Lambda_h\mu_v - \gamma\psi\epsilon\Lambda_h\mu_v}.$$

Hence, the control reproduction number is given by

$$\mathcal{R}_c = \sqrt{\frac{a_3b^2\kappa\tau\mu_h p_h p_m\Lambda_v\left((1-\alpha)\omega+\mu_h\right)}{\Lambda_h\mu_v^2a_1a_2a_3a_4\left(1-\Phi\right)\left((1-\alpha)\omega+\mu_h+\nu_1\right)}} \quad \text{where} \quad \Phi = \frac{\gamma\psi\varepsilon}{a_2a_3} < 1. \tag{6}$$

As a result, the following theorem holds according to [37].

Theorem 3
The $\mathcal{E}_0$ of system (1) is locally asymptotically stable if $\mathcal{R}_c < 1$ and is unstable if $\mathcal{R}_c > 1$.

2.3. Endemic equilibrium

Here, we determine the endemic equilibrium for system (1) denoted by
$\mathcal{E}^* = (S_h^*, E_h^*, I_h^*, L_h^*, V_h^*, S_v^*, E_v^*, I_v^*)$. In order to obtain the endemic equilibrium $\mathcal{E}^*$, we set the left-hand side of system (1) to zero and solve the resulting system of equations as follows

$$\begin{cases} 0 &= \Lambda_h - p_h\lambda^*S_h^*I_v^* + \delta L_h^* + (1-\epsilon)\gamma I_h^* + (1-\alpha)\omega V_h^* - (\mu_h+v_1)S_h^*, \\ 0 &= p_h\lambda^*(S_h^*+L_h^*)I_v^* - a_1E_h^*, \\ 0 &= \tau E_h^* + \psi L_h^* - a_2I_h^*, \\ 0 &= \varepsilon\gamma I_h^* - p_h\lambda^*L_h^*I_v^* - a_3L_h^*, \\ 0 &= v_1S_h^* + v_2L_h^* - (1-\alpha)\omega V_h^* - \mu_hV_h^*, \\ 0 &= \Lambda_v - p_m\lambda^*S_v^*I_h^* - \mu_vS_v^*, \\ 0 &= p_m\lambda^*S_v^*I_h^* - a_4E_v^*, \\ 0 &= \kappa E_v^* - \mu_vI_v^*, \end{cases} \tag{7}$$

where $\lambda^* = b/N_h^*$. For simplicity's sake, expressing $\mathcal{E}^*$ in terms of λ^*. From the last equation of system (7), we obtain

$$E_v^* = \frac{\mu_vI_v^*}{\kappa}. \tag{8}$$

Adding the sixth and seventh equations of system (7) and solving for S_v^* gives

$$S_v^* = \frac{\kappa\Lambda_v - a_4\mu_vI_v^*}{\kappa\mu_v}. \tag{9}$$

Substituting expressions (8) and (9) into the seventh equation of (7) and solving for I_h^* gives

$$I_h^* = \frac{a_4\mu_v^2I_v^*}{p_m\lambda^*\left(\kappa\Lambda_v - a_4\mu_vI_v^*\right)}. \tag{10}$$

Substituting (10) into the fourth equation of (7) and solving for L_h^* gives

$$L_h^* = \frac{\gamma\varepsilon a_4\mu_v^2 I_v^*}{p_m\lambda^*\left(a_3 + p_h\lambda^* I_v^*\right)\left(\kappa\Lambda_v - \mu_v a_4 I_v^*\right)}. \tag{11}$$

Substituting (10) and (11) into the third equation of (7) and solving for E_h^* gives

$$E_h^* = \frac{a_4\mu_v^2 I_v^*\left(a_2 p_h\lambda^* I_v^* + a_2 a_3\left(1-\Phi\right)\right)}{\tau p_m\lambda^*\left(a_3 + p_h\lambda^* I_v^*\right)\left(\kappa\Lambda_v - a_4\mu_v I_v^*\right)}. \tag{12}$$

Substituting (11) and (12) into the second equation of system (7) and solving for S_h^* gives

$$S_h^* = \frac{a_4\mu_v^2\left(p_h\lambda^* I_v^*\left(a_1a_2 - \gamma\tau\varepsilon\right) + a_1a_2a_3(1-\Phi)\right)}{\lambda^{*^2}\tau p_h p_m\left(a_3 + p_h\lambda^* I_v^*\right)\left(\kappa\Lambda_v - a_4\mu_v I_v^*\right)}. \tag{13}$$

Substituting (13) and (11) into the fifth equation of (7) and solving for V_h^* gives

$$V_h^* = \frac{a_4\mu_v^2\left(a_1a_2v_1\left(p_h\lambda^* I_v^* + a_3(1-\Phi)\right) + \gamma\tau\varepsilon p_h\left(v_2 - v_1\right)\lambda^* I_v^*\right)}{\tau p_h p_m\lambda^{*^2}\left((\alpha-1)\omega - \mu_h\right)\left(a_3 + p_h\lambda^* I_v^*\right)\left(a_4 I_v^*\mu_v - \kappa\Lambda_v\right)}. \tag{14}$$

Notice that equations (8) - (14) are expressed in terms of I_v^*. Thus, substituting (8) - (14) into the first equation of system (7) leads to the following second-order polynomial in terms of I_v^*,

$$\xi_2\left(I_v^*\right)^2 + \xi_1 I_v^* + \xi_0 = 0, \tag{15}$$

where

$$\begin{aligned}
\xi_0 &= a_1a_2a_4\mu_h\mu_v^2\left((1-\alpha)\omega + \mu_h + \nu_1\right)\left(1-\Phi\right)\left(\mathcal{R}_e - 1\right),\\
\xi_1 &= \lambda^* p_h(a_4\mu_v(a_3((\alpha-1)\omega - \mu_h)(\mu_v(\gamma\tau(\epsilon-1) + a_1a_2(1-\Phi)) + \lambda^*\tau\Lambda_h p_m) + \mu_v(((1-\alpha)\gamma\delta\tau\omega\epsilon)\\
&\quad +(1-\alpha)\gamma\nu_2\tau\omega\epsilon + \mu_h(a_1a_2((\alpha-1)\omega - \mu_h - \nu_1) + \gamma\tau\varepsilon(-\alpha\omega + \delta + \mu_h + \nu_1 + \omega))))\\
&\quad +\kappa\lambda^{*^2}\tau\Lambda_h p_h p_m\Lambda_v(-\alpha\omega + \mu_h + \omega)),\\
\xi_2 &= -a_4\lambda^{*^2}p_h^2\mu_v\left((1-\alpha)\omega + \mu_h\right)\left(\mu_v\left(\left(\mu_d + \mu_h\right)\left(\mu_h + \tau\right) + \gamma\mu_h\right) + \lambda^*\tau\Lambda_h p_m\right),
\end{aligned} \tag{16}$$

with

$$\mathcal{R}_e = \left[\left(\frac{\lambda^*\Lambda_h}{b\mu_h}\right)\mathcal{R}_c\right]^2. \tag{17}$$

We note from (16) that

$$\xi_0 > 0 \quad \text{when} \quad \mathcal{R}_e > 1 \quad \text{or} \quad \xi_0 < 0 \quad \text{when} \quad \mathcal{R}_e < 1.$$

Also, note that there is a possibility that either $\xi_1 > 0$ or $\xi_1 < 0$. Lastly, it can be clearly noted that $\xi_2 < 0$. Thus, we have the following results on the existence of $\mathcal{E}^*$ of system (1).

Theorem 4
The following results hold.

(E1) Model (1) has no endemic equilibrium when $\mathcal{R}_e < 1$ and $\xi_1 < 0$.
(E2) Model (1) has a unique endemic equilibrium for the following possible conditions;
  1. $\mathcal{R}_e > 1$ and $\xi_1 > 0$,
  2. $\mathcal{R}_e > 1$ and $\xi_1 < 0$.
(E3) Model system (1) has two endemic equilibria when $\mathcal{R}_e < 1$ and $\xi_1 > 0$.

Biological and Public-Health Interpretation of Theorem 4

Theorem 4 indicates that the vaccination relapse model may admit zero, one, or two endemic equilibria depending on the interplay between the effective reproduction number $\mathcal{R}_e$, the relapse-related term ξ_1, and the transmission parameters. These mathematical outcomes have clear biological and public-health implications for malaria control in Lembata Regency.

- **Case (E1): No endemic equilibrium when $\mathcal{R}_e < 1$ and $\xi_1 < 0$.** This result suggests that malaria transmission cannot be sustained when the effective reproduction number is brought below unity, and relapse-driven reinfection is sufficiently suppressed. *Public-health implication:* if relapse is well controlled and vaccination effectively reduces susceptibility, malaria elimination is achievable even without additional interventions.
- **Case (E2): A unique endemic equilibrium when $\mathcal{R}_e > 1$.** When transmission remains above the threshold for sustained transmission, the system settles into a single endemic state. *Public-health implication:* persistent malaria transmission will continue unless strong interventions (e.g., vaccination, relapse reduction, vector control) reduce $\mathcal{R}_e$ below one.
- **Case (E3): Two endemic equilibria when $\mathcal{R}_e < 1$ but $\xi_1 > 0$.** This scenario is of particular biological interest, as it suggests the possibility of backward bifurcation. Even when $\mathcal{R}_e < 1$, malaria may persist at a low endemic level due to relapse-driven reinfection. *Public-health implication:* partial vaccination or partial relapse control may "trap" the population in a low-level endemic state. Elimination requires not only reducing $\mathcal{R}_e$ below one but also achieving sufficiently high vaccination coverage and relapse suppression. Incremental improvements may not be enough for elimination in Lembata Regency.

3. Mathematical model with two types of treatment

We extend the Model (1) to include two types of treatment: that is, radical cure and bloodstream treatments. The state variables S_h, E_h, I_h, L_h, S_v, E_v, and I_v have the same interpretations as in the first model with vaccination only. The extended model includes the following additional human compartments: T_b represents the class of individuals receiving bloodstream treatments and T_r is the class of individuals receiving radical cure treatment. A complete cure for malaria requires a combination therapy that addresses both the blood stage and liver stage of the parasites, effectively eliminating all parasites from the body. For the blood stage treatment, Chloroquine is commonly used; however, in regions where Chloroquine resistance is prevalent, artemisinin-based combination therapy is employed to clear the blood stages of the parasites. The radical cure, also known as a radical treatment, specifically refers to the complete elimination of malaria parasites from the body, including the elimination of dormant liver-stage parasites known as hypnozoites, which are found in Plasmodium vivax and Ovale infections [7, 19]. The descriptions of the new parameters are given in Table 2.

Table 2. Parameter description of the model with two types of treatment.

Parameter	Description
θ	Treatment rate
p	Proportion of T_r individuals who progress to the susceptible class
ε_t	Proportion of symptomatic infected individuals who receive bloodstream treatments

Figure 2 shows the interactions between human and mosquito populations in the context of malaria infection and treatment strategies. Combining Figure 2 with the new parameters and state variables' descriptions gives:

$$\begin{cases} \dfrac{dS_h}{dt} = \Lambda_h - \dfrac{bp_h S_h I_v}{N_h} - \mu_h S_h + \delta L_h + \gamma T_b + p\gamma T_r, \\ \dfrac{dE_h}{dt} = \dfrac{bp_h(S_h + L_h) I_v}{N_h} - (\mu_h + \tau) E_h, \\ \dfrac{dI_h}{dt} = \tau E_h + \psi L_h - (\theta + \mu_h + \mu_d) I_h, \\ \dfrac{dT_r}{dt} = (1 - \varepsilon_t)\theta I_h - (\mu_h + \gamma) T_r, \\ \dfrac{dT_b}{dt} = \varepsilon_t \theta I_h - (\mu_h + \gamma) T_b, \\ \dfrac{dL_h}{dt} = (1 - p)\gamma T_r - \dfrac{bp_h L_h I_v}{N_h} - (\mu_h + \psi + \delta) L_h, \\ \dfrac{dS_v}{dt} = \Lambda_v - \dfrac{bp_m S_v (I_h + T_r + T_b)}{N_h} - \mu_v S_v, \\ \dfrac{dE_v}{dt} = \dfrac{bp_m S_v (I_h + T_r + T_b)}{N_h} - (\kappa + \mu_v) E_v, \\ \dfrac{dI_v}{dt} = \kappa E_v - \mu_v I_v, \end{cases} \tag{18}$$

with initial conditions

$$S_h(0) > 0,\ E_h(0) \geq 0,\ I_h(0) \geq 0,\ T_r(0) \geq 0,\ T_b(0) \geq 0,\ L_h(0) \geq 0,\ S_v(0) > 0,\ E_v(0) \geq 0,\ I_v(0) \geq 0$$

where all the model parameters are assumed to be positive. Results on positivity and boundedness of solutions for system (18) can be obtained using a similar approach carried out for model system (1). We now establish the disease-free equilibrium and control reproduction number for system (18).

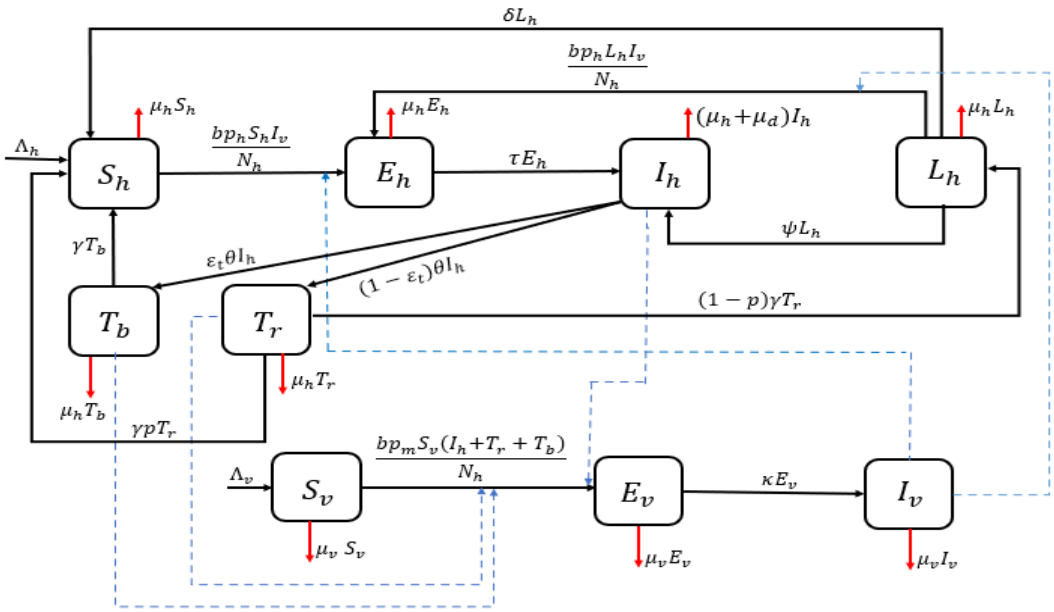

Figure 2. Model flow chart with two types of treatments.

3.1. *Disease-free equilibrium and the reproduction number of system* (18)

We first establish the disease-free equilibrium, a state depicting the absence of disease. The disease-free equilibrium for system (18) is given by

$$\mathcal{E}_1 = \left(S_h^1, E_h^1, I_h^1, T_r^1, T_b^1, L_h^1, S_v^1, E_v^1, I_v^1\right) = \left(\frac{\Lambda_h}{\mu_h}, 0, 0, 0, 0, 0, \frac{\Lambda_v}{\mu_v}, 0, 0\right).$$

We derive the control reproduction number of the model using the concept of the next generation matrix [37] and obtain

$$\mathcal{R}_0^t = \sqrt{\frac{\bar{a}_4 b^2 \kappa \tau \left(\bar{a}_3 + \theta\right) \mu_h p_h p_m \Lambda_v}{\Lambda_h \mu_v^2 \bar{a}_1 \bar{a}_2 \bar{a}_3 \bar{a}_4 \bar{a}_5 \left(1 - \Phi_t\right)}} \quad \text{where} \quad \Phi_t = \frac{\gamma\theta(1-p)\psi\left(1-\varepsilon_t\right)}{\bar{a}_2 \bar{a}_3 \bar{a}_4} < 1. \tag{19}$$

(See Appendix 1 for proof). The following theorem follows

Theorem 5
The $\mathcal{E}_1$ of model system equations (18) is locally asymptotically stable if $\mathcal{R}_0^t < 1$ and is unstable if $\mathcal{R}_0^t > 1$.

3.2. *Global stability of the malaria-free equilibrium*

Theorem 6
The malaria-free equilibrium is globally asymptotically stable if $\mathcal{R}_0 < 1$.

The proof of this theorem is given in Appendix 2.

3.3. *Endemic equilibrium for the model with two types of treatment*

For the endemic equilibrium of model (2), see Appendix 3. The following results hold.

Theorem 7

(EE1) System (18) has no endemic equilibrium when $\mathcal{R}_e^t < 1$ and $\chi_1 > 0$.
(EE2) System (18) has a unique endemic equilibrium for the following possible conditions;
  1. $\mathcal{R}_e^t > 1$ and $\chi_1 < 0$,
  2. $\mathcal{R}_e^t > 1$ and $\chi_1 > 0$.
(EE3) System (18) has two endemic equilibria when $\mathcal{R}_e^t < 1$ and $\chi_1 < 0$.

Biological and Public-Health Interpretation of Theorem 7

Theorem 7 shows that the extended model incorporating radical cure and bloodstream treatment may also exhibit zero, one, or two endemic equilibria. These cases correspond to important public-health considerations for *Plasmodium vivax* control.

- **Case (EE1): No endemic equilibrium when $R_t^e < 1$ and $\chi_1 > 0$.** When treatment is sufficiently effective, particularly when radical cure successfully clears hypnozoites, the system cannot sustain malaria transmission. *Public-health implication:* effective radical cure programs, paired with timely treatment of bloodstream infections, can interrupt transmission even in relapse-prone settings.
- **Case (EE2): A unique endemic equilibrium when $R_t^e > 1$.** This case reflects the typical endemic malaria situation where treatment coverage or treatment success is insufficient. *Public-health implication:* improving treatment access, drug supply reliability, and timely diagnosis is essential for reducing R_t^e below one.
- **Case (EE3): Two endemic equilibria when $R_t^e < 1$ but $\chi_1 < 0$.** As in Model 1, this indicates the possibility of backward bifurcation. High relapse frequency or insufficient radical cure may sustain transmission despite an R_t^e value below unity. *Public-health implication:* malaria may persist even under apparently strong treatment interventions. Achieving high radical cure coverage and improving adherence are crucial for shifting the system toward elimination.

4. Numerical simulations

Table 3. Transition rates for our model parameters used for numerical simulations. The letters H and V stand for humans and vectors, respectively, which in this case are mosquitoes.

Parameter	Range/Values	Units	Refs.
Λ_h	$\left[\frac{2000000}{12\times65} - \frac{250000}{12\times65}\right]\frac{2340000}{12\times65}$	$H \times Month^{-1}$	Estimated
μ_h	$\left[\frac{1}{70\times65} - \frac{1}{71.5\times65}\right]\frac{1}{65\times12}$	Month^{-1}	[1],[34]
δ	1	Month^{-1}	Assumed
b	30.8	$H \times (V \times Month)^{-1}$	Assumed
p_h	0.5	Unitless	Fitting
τ	5×10^{-5}	Month^{-1}	Fitting
γ	$5.5 \times 12 \times 10^{-4}$	Month^{-1}	Assumed
ψ	5.9	Month^{-1}	Fitting
μ_d	$30 \times 1.9 \times 10^{-5}$	Month^{-1}	[29]
α	(0,1) 0.88	Unitless	Varied
Λ_v	10000	$V \times Month^{-1}$	Estimated
p_m	0.17	Unitless	Fitting
κ	$\frac{12}{30}\left[\frac{10}{30} - \frac{14}{30}\right]$	Month^{-1}	[33, 30, 16]
μ_v	$\frac{30}{21}$	Month^{-1}	[27, 2]
θ	0.5 (0,1)	Month^{-1}	Assumed
ε_t	0.5 (0,1)	Unitless	Assumed
p	0.45 (0,1)	Unitless	Assumed

4.1. Model parameter estimation

The model's parameter values were estimated using malaria incidence data from Lembata Regency in East Nusa Tenggara Province, Indonesia. We use the methods proposed in Chowel *et al.* [13] to calibrate our model (1) parameters. The parameter values for p_h, p_m, τ, and ψ were estimated from the fitting process. Additionally, the parameter ψ supported by [32]. In malaria vaccine research and development, various factors influence the duration and effectiveness of immunity conferred by vaccines. Clinical trials have revealed differing durations of protection, exemplified by the RTS,S/AS01 (RTS,S) vaccine, which provides partial protection requiring multiple doses and boosters for sustained efficacy in children and infants. Individual immune responses vary due to factors like age, health status, and genetic diversity, impacting the strength and longevity of vaccine-induced immunity. Considering these complexities, specific parameters ($\nu_1 = 0.3, \nu_2 = 0.5, \omega = 0.5$) related to vaccination and the latent malaria classes, each normalized Month^{-1} are assumed as our model attains an endemic equilibrium trajectory. We point out that the remaining parameters for the model (1) are taken from published literature, and some are assumed as summarized in Table 3.

The parameters for Model (1) were estimated by fitting the model-generated monthly incidence curve to the reported malaria incidence from Lembata Regency. Following the approach of Chowell [13], we calibrated the model by minimizing a nonlinear least-squares objective function that measures the discrepancy between the observed data and the model predictions. In this study, the parameters estimated from the data are p_h, p_m, τ, ψ which together constitute the parameter vector Φ. Let y_i denote the observed incidence at month i, and let $\hat{y}_i(\Phi)$ denote the model-predicted incidence. The parameter estimates were obtained by minimizing

$$\mathcal{L}(\Phi) = \sum_{i=1}^{n} \left(y_i - \hat{y}_i(\Phi)\right)^2,$$

using MATLAB's `lsqnonlin` nonlinear least-squares solver. Parameter uncertainty for the estimated vector $\Phi = (p_h, p_m, \tau, \psi)$ was quantified using a nonparametric bootstrap procedure. We generated 1,000 synthetic

datasets by resampling the residuals and refitted the model to each dataset. The empirical distributions of the resulting parameter estimates were then used to compute 95% confidence intervals, as shown in Figure 4. These intervals also provide insight into parameter identifiability. Narrower intervals correspond to well-identified parameters, whereas broader intervals reflect structural or observational uncertainty, particularly for relapse-related quantities derived from aggregated incidence data. The resulting figures, which show the line of best fit in red and the blue circle representing the data points shown in Figure 3 with the distribution of the estimated parameters (p_h, p_m, τ, and ψ) in Figure 4.

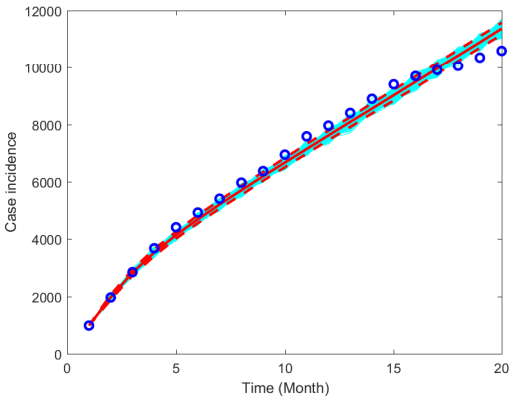

Figure 3. Numerical fitting of the model (1) showing the line of best fit, which is generated with the 95% confidence interval for malaria incidence data from Lembata Regency, East Nusa Tenggara Province, Indonesia.

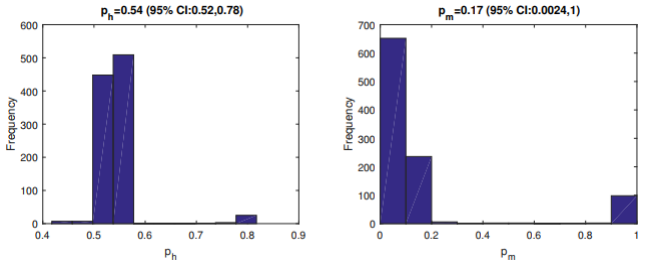

(a)

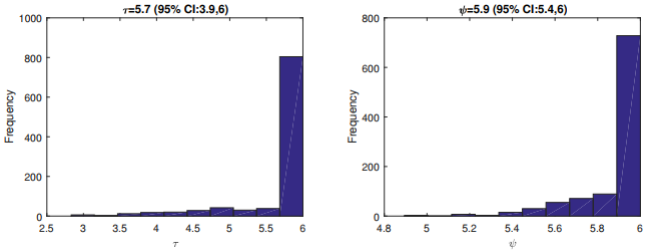

(b)

Figure 4. Frequency distribution for parameters p_h, p_m, τ, and ψ indicating their mean values respectively generated with the 95% confidence interval.

4.2. Global sensitivity analysis

In this subsection, we explore the influential parameters on the reproduction number, $\mathcal{R}_c$, for the malaria model (1) with vaccination interventions. We use the combination of Latin Hypercube Sampling and the Partial Rank Correlation Coefficients (PRCCs) as in Blower *et al.* [11] to establish the most influential parameters through global sensitivity analysis. This method generates PRCC values to help determine parameters with low or high variability responsible for deriving malaria infection and, as a result, guides policy-making on the type of interventions required to control malaria spread. This was achieved with 1000 simulations for each run and a step unit of 1, considered within a 95% confidence interval as carried out in RStudio software. The mean value of each parameter PRCC value is plotted and shown in Figure 5 below.

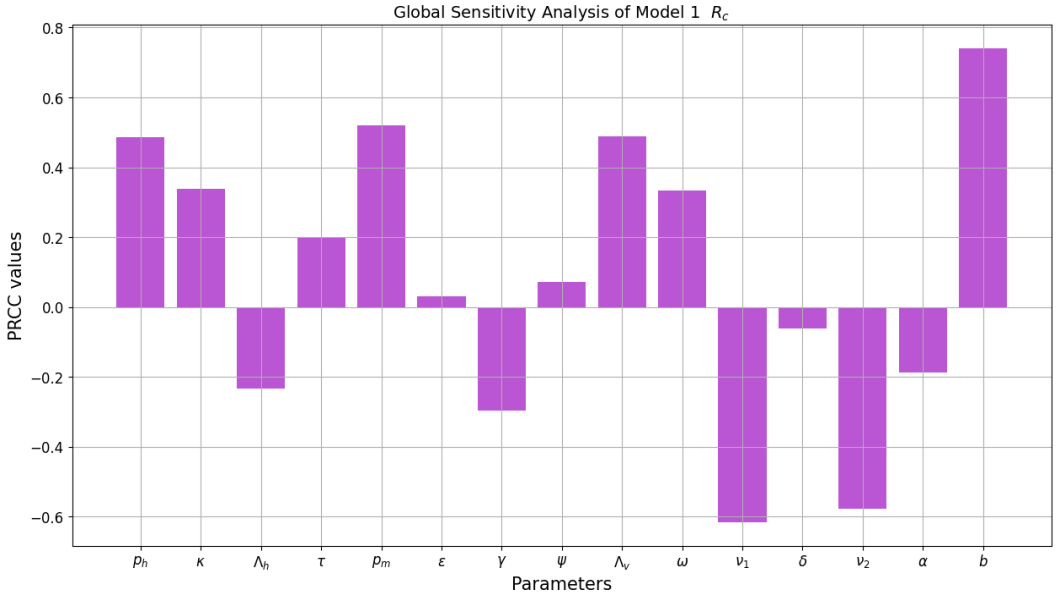

Figure 5. Tornado plot indicating the PRCC values for the model parameters contained in the control reproduction number of the model (1). Parameters such as mortality rates were excluded from our analysis as their variability can not be controlled in a real-life scenario.

Additionally, a positive PRCC indicates that increasing the parameter of interest subsequently leads to an increase in $\mathcal{R}_c$, thereby promoting endemicity. In contrast, those parameters with negative PRCC suggest that increasing the parameter of interest decreases the $\mathcal{R}_c$, therefore stimulating a disease-free steady state. A clear look at Figure 5, indicate that the parameters p_h , p_m, Λ_v and b have strong positive PRCCs values while ν_1, ν_2 have strong negative PRCCs against $\mathcal{R}_c$. We aim to implement control measures that target promoting ν_1, ν_2 while targeting to reduce the transmission rates p_h , p_m, Λ_v and b to reduce Malaria spread in Lembata Regency, East Nusa Tenggara Province, Indonesia. These parameters of interest will be investigated in our numerical results for the remainder part of the manuscript, especially the simulation of the second Malaria model, which incorporates treatment rates as well as the radical/bloodstream treatment rates to fully understand the underlying dynamics while suggesting control interventions that will be effective in fighting the spread of malaria in the endemic region, such as Indonesia. Similar modeling analysis for other epidemic models has been carried out for malaria [35, 23, 36], coronavirus [20], listeriosis [15], schistosomiasis [26], HIV/AIDS-Listeriosis co-dynamics [14], for an interested reader.

4.3. Existence of local stability

Figure 6 illustrates the local stability of $\mathcal{E}_0$ as presented in Theorem 3.

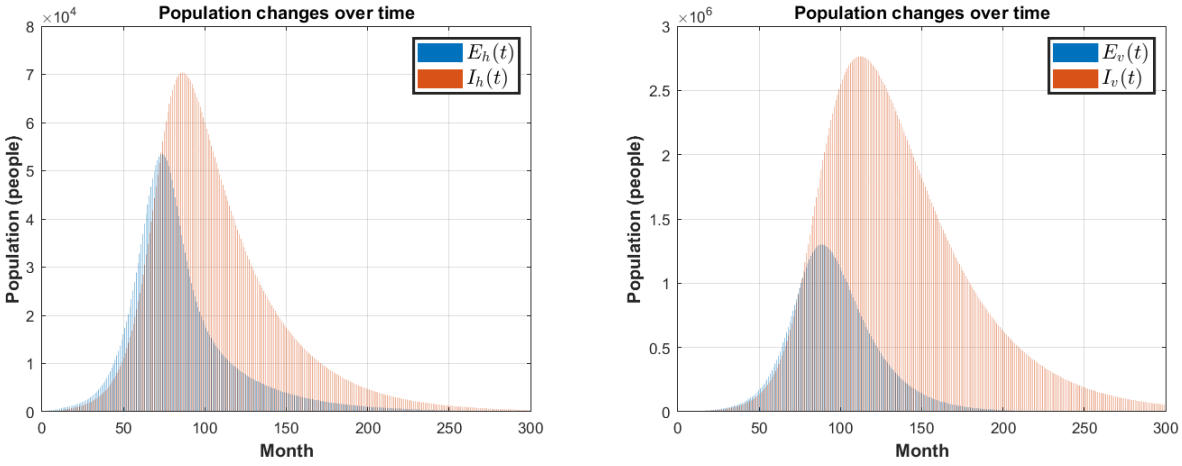

Figure 6. General population trajectory for (a) exposed and infected humans and (b) exposed and infected mosquitoes when $\mathcal{R}_0 = 0.6382 < 1$.

4.4. Impact of treatment strategy

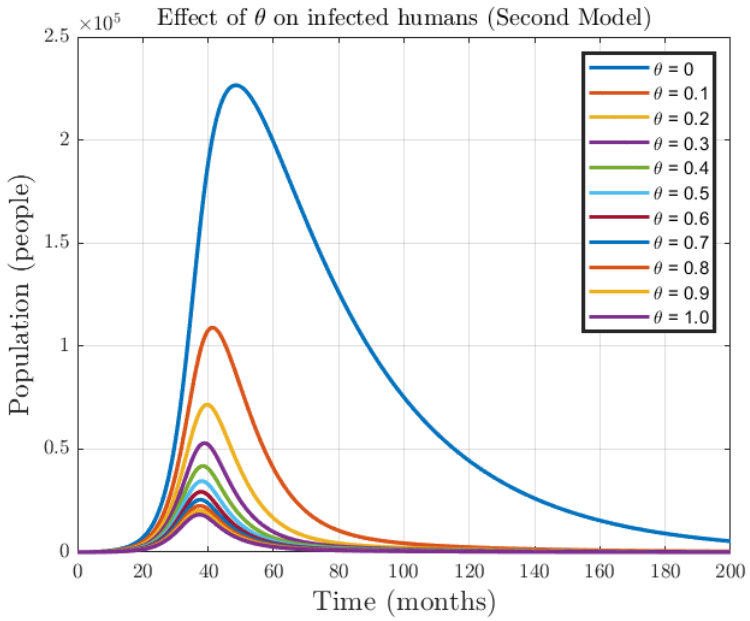

Figure 7. Effects of varying the parameter θ on infected humans $I_h(t)$.

Figure 7 is simulated using the second model system (18) with two types of treatment, that is, radical treatment and bloodstream treatment. The graph shows that radical treatment of infected individuals is indeed important in the fight against malaria infection.

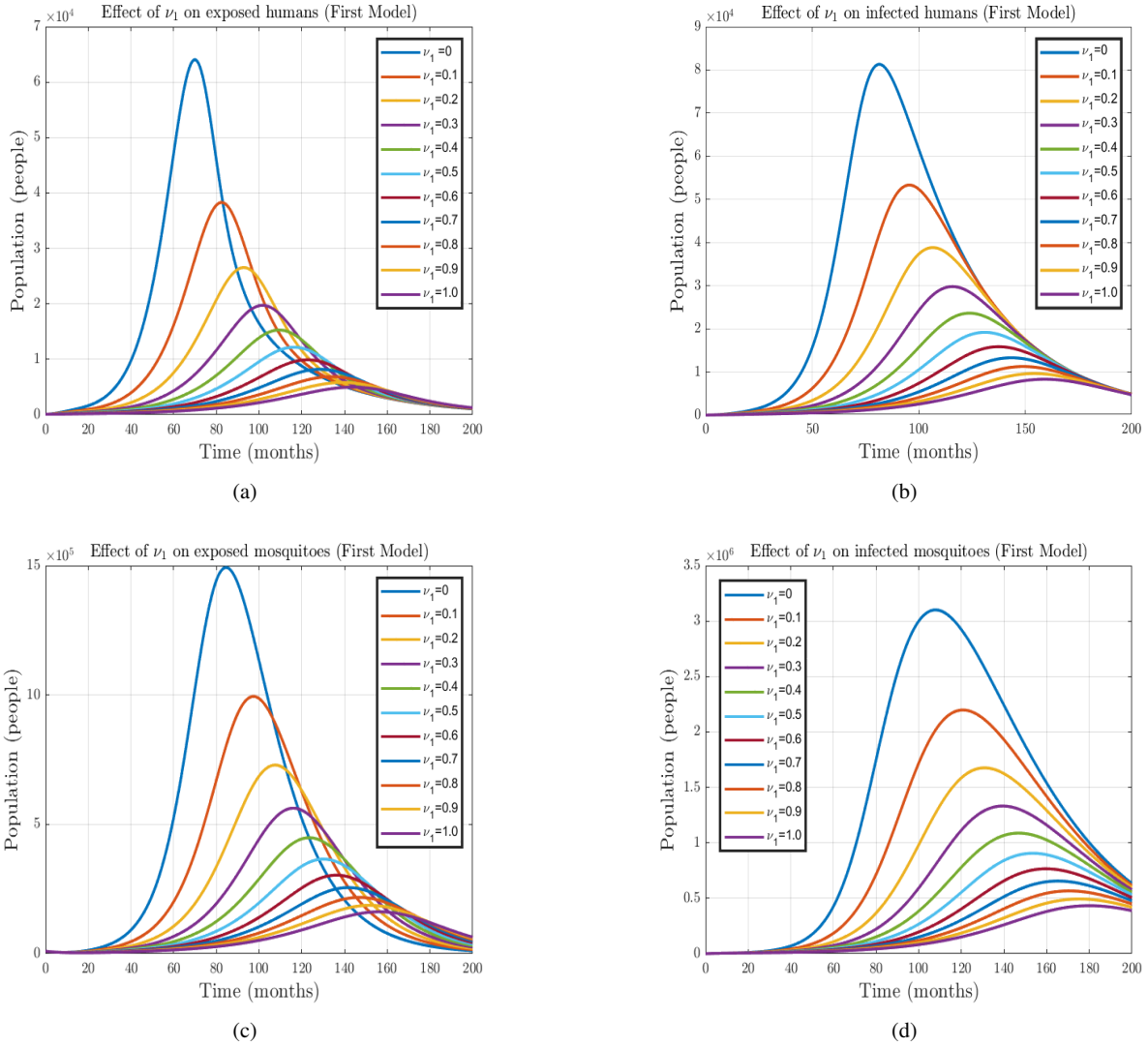

Figure 8. Effects of varying the parameter ν_1, on the population changes of (a) exposed humans $E_h(t)$, (b) infected humans $(I_h(t))$, (c) exposed mosquitoes $(E_v(t))$ and (d) infected mosquitoes $(I_v(t))$.

Figure 8 is simulated using the first model system (1) with vaccination. The graph illustrates the impact of varying the parameter ν_1, on the population changes of exposed humans, $E_h(t)$, infected humans, $I_h(t)$, exposed mosquitoes, $E_v(t)$ and infected mosquitoes $I_v(t)$. This shows that vaccination is useful in reducing the prevalence of malaria infections.

4.5. Assessing the impact of transmission rates on malaria dynamics

Figure 9(a) demonstrates that as treatment rate (θ) increases, there is a sharp decline in the numerical values of $\mathcal{R}_c^t$. The decrease is gradual for values of approximately $\theta < 0.5$, while when $\theta > 0.5$, the reduction becomes more pronounced. Treatment success is particularly effective at reducing the control reproduction number once it goes beyond the 50% threshold mark, as indicated in the magenta-colored line. Additionally, the numerical value for reproduction number $\mathcal{R}_c^t$ goes below unity when the value of the treatment rates is approximately $\theta > 0.51$.

Therefore, it is clear that 50% will be required to lower the $\mathcal{R}_c^t < 1$, which is sufficient to lead to malaria eradication in Lembata Regency, East Nusa Tenggara Province, Indonesia. The results depicted in Figure 9(b) can also be interpreted in a similar fashion for varying the relapse rate on $\mathcal{R}_c$ but with an inverse relationship against $\mathcal{R}_c$. The second result suggests that as more individuals relapse, this will result in malaria endemicity. Hence, this parameter is of public health concern, and control measures should target reducing the relapse rate and its associated causes in the human population. The variation in the treatment rate θ and the relapse parameter ψ was selected based on biologically plausible ranges reported in the malaria modeling literature and on the values estimated from our calibration to Lembata Regency data. These ranges were chosen to capture both the lower and upper bounds of feasible intervention performance under local conditions. The independent variation of parameters was used to examine the isolated sensitivity of the control reproduction number to each intervention lever without confounding effects introduced by simultaneous parameter changes. This approach helps identify which single parameters exert the strongest influence on malaria persistence, thereby providing a clearer understanding of the relative importance of treatment coverage and relapse control for malaria elimination efforts in the region.

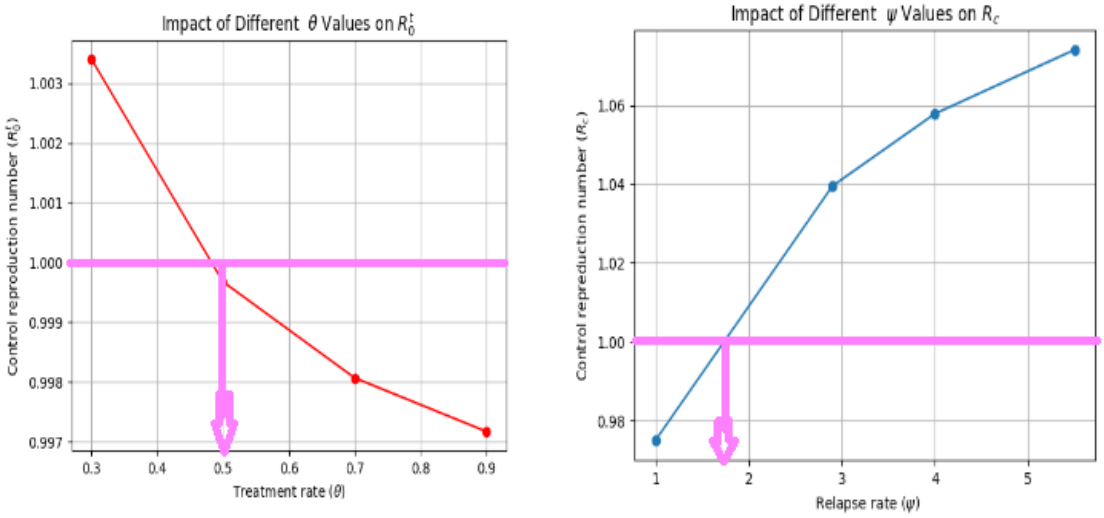

(a) (b)

Figure 9. Varying: (a) the treatment θ, and (b) the relapse rate control reproduction numbers $\mathcal{R}_c$ and $\mathcal{R}_c^t$ respectively. In this simulation analysis, the parameter values for θ and ψ were varied while the remaining parameters, as defined in Table 3, were kept constant.

We simulate the impact of the transmission parameter's relapse rate, vaccination rates, and proportion of asymptomatic infected individuals to investigate its impact on the control reproduction number. This is of great importance as it helps public health policymakers guide the rules to mitigate the spread of malaria after assessing the impact of these rates. Figure 10(a) depicts an increase in the relapse rate increases the control reproduction number, whereas an increase in the vaccination rate decreases the control reproduction number, $\mathcal{R}_c$. The biological implication of these results suggests that it is beneficial to increase vaccination rates to help avert the emergence of new infectious individuals and help, in turn, reduce malaria spread. Looking at Figure 10(b), a similar interpretation of the results can also be explained only by the fact we simulate the recovery rate and proportion of infected individuals on $\mathcal{R}_c^t$.

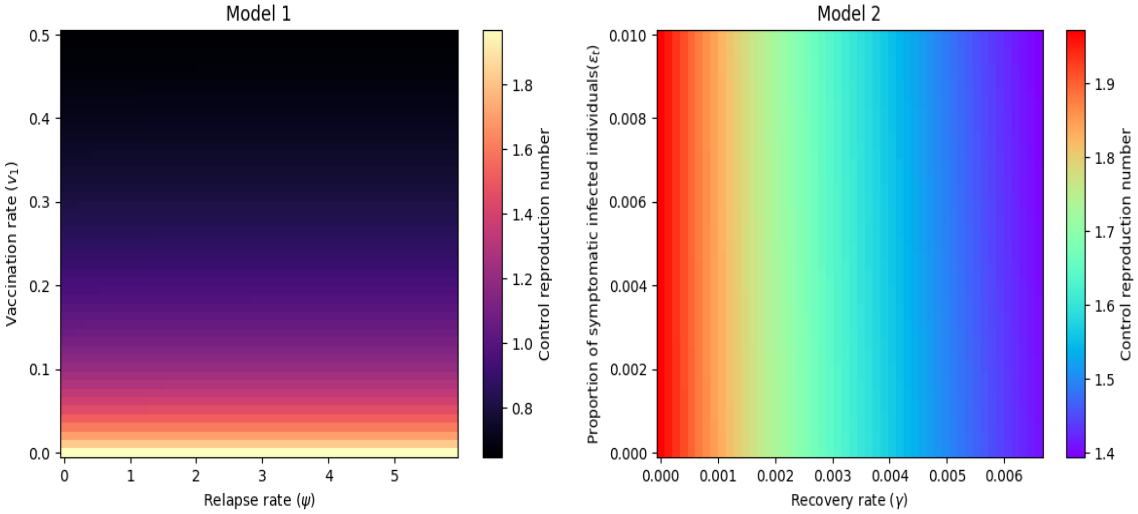

(a) (b)

Figure 10. Numerical results showing a heat map plot for the control reproduction number $\mathcal{R}_c$ and $\mathcal{R}_c^t$ respectively, as a function of vaccination (ν_1) and relapse (ψ) rates. The remaining parameters are kept constant as defined in Table 3.

Figure 10 presents heat maps illustrating how different combinations of treatment coverage and relapse-related parameters affect the control reproduction number. While these thresholds provide useful theoretical benchmarks, it is important to consider their practical feasibility within the health system context of East Nusa Tenggara Province. For example, the model suggests that achieving a treatment rate of approximately 50% or higher is required to drive R_0^t below one. In practice, however, reaching such levels may be challenging due to limited healthcare infrastructure, geographic barriers between islands, inconsistent drug availability, and delays in diagnosis and treatment. These operational constraints imply that achieving the model-identified thresholds requires strengthened health-system capacity, more reliable antimalarial supply chains, and expanded community-based treatment programs. Therefore, the heat-map results should be interpreted as idealized targets that indicate where the greatest potential for intervention gains lies, rather than as immediately attainable thresholds under current regional conditions.

5. Discussions and Conclusions

5.1. Discussions

In this paper, two malaria models were formulated to assess the impact of vaccination and treatment on malaria control. Data for malaria incidence from Lembata Regency, East Nusa Tenggara Province, Indonesia, were used to validate the developed models and perform parameter estimation. Both models subdivide the human and mosquito populations into different categories with respect to malaria infection. The first model incorporates vaccination of susceptible individuals together with individuals in the latency stage of infection. The disease-free equilibrium is shown to be locally asymptotically stable whenever the reproduction number of the model is less than the unit, that is $\mathcal{R}_0 < 1$. Some conditions that guarantee the existence of the endemic equilibrium $\mathcal{E}^*$ are established. The second model includes two treatment types, namely, radical cure and bloodstream treatments. A similar theoretical analysis is carried out for the second model. It is also shown that the disease-free equilibrium of this model is locally asymptotically stable whenever the model reproduction number is less than one, that is, $\mathcal{R}_0^t$. Some conditions that guarantee the endemic equilibrium $\mathcal{E}^\bullet$ are established. Numerical simulations for both models are carried out using

the MATLAB programming language. The results show that vaccination and treatment play a crucial role in the fight against malaria infection.

We note that the models developed in this study have certain limitations. One of the limitations of our models, particularly the first, is that it assumes that all susceptible individuals are eligible for the vaccine, which is not the case for the only malaria vaccine currently available. This vaccine is designed for children under the age of 5 and is given in four doses. Taking into account the age group and the number of doses will be a major improvement in our work and will be the subject of future investigation. Our numerical results show that a treatment rate above $\theta > 0.51$ is needed to bring the control reproduction number below one. While this finding offers a clear theoretical benchmark, achieving this level of treatment coverage in East Nusa Tenggara Province (ENTP) is far more complex in practice. ENTP is a geographically fragmented region with limited healthcare infrastructure, variable access to clinics, and occasional shortages of antimalarial drugs. These realities mean that simply increasing treatment rates is not only a medical challenge but also a logistical one. Reaching the threshold $\theta > 0.51$ would require a steady and reliable drug supply, timely diagnosis, stronger community outreach, and sufficient healthcare personnel, factors that are not guaranteed in many parts of the province. Although our mathematical model does not explicitly account for these operational barriers, the results highlight an important point: improving treatment systems, strengthening supply chains, and supporting community-level health workers are essential steps if the benefits predicted by the model are to be realized. This emphasizes the need for public health strategies that pair mathematical insights with the on-the-ground realities of malaria control in ENTP.

5.2. Comparison with Existing Literature

Mathematical modeling studies have explored malaria transmission dynamics in Indonesia, including the work of Handari *et al.* [23], who examined the impact of the RTS,S vaccine and transmission-blocking drugs in Papua and West Papua. While their framework incorporates vaccination, it differs from our approach in both structure and purpose. Their model focuses on vaccine-induced reductions in the force of infection in regions where RTS,S implementation efforts are underway, whereas our vaccination model serves as a generalized exploratory scenario for Lembata Regency, where the vaccine is not yet widely available. Other studies, such as Fatmawati *et al.* [39], have incorporated seasonal forcing and optimal control to model malaria transmission in Papua, highlighting the role of environmental variability. In East Nusa Tenggara Province specifically, previous research has centered on malaria awareness, prevalence patterns, and local risk factors rather than mechanistic transmission dynamics; for example, Guntur *et al.* [40] examined awareness levels across endemic settings, while more recent observational studies have documented long-term prevalence trends [41] and identified key malaria risk factors among rural and hilly communities in the region [42]. These works provide valuable epidemiological context but do not offer dynamic modeling frameworks tailored to ENTP. By contrast, our models were intentionally designed to be tractable and compatible with the limited surveillance data available for Lembata. The contribution of this study lies in providing a focused analysis of relapse, treatment, and hypothetical vaccination pathways using the only accessible dataset for the region, thereby complementing rather than replicating existing modeling efforts in Indonesia.

5.3. Strengthen Limitations and Future Work

In our model, individuals in both the susceptible and latent compartments are allowed to receive vaccination. This choice reflects a simplifying assumption rather than a literal representation of how malaria vaccines are deployed in practice. The RTS,S vaccine is primarily administered to young children and does not target latent *Plasmodium vivax* infections. In the context of our model, vaccinating the latent class should therefore be interpreted as a theoretical mechanism for reducing future susceptibility and strengthening overall population immunity in a setting where relapse contributes substantially to ongoing transmission.

There are, however, important limitations to this simplified vaccination strategy. The model does not include age structure, even though real-world vaccination programs are age-restricted and vaccine-induced immunity differs across demographic groups. Incorporating age structure would enable the model to more accurately capture childhood vaccination schedules, heterogeneous immunity, and variations in clinical vulnerability. Such an

extension would likely alter the quantitative results, particularly the estimated thresholds required for vaccination to significantly reduce transmission in Lembata Regency.

Similarly, the current model assumes a single-dose protective effect, whereas RTS,S requires multiple doses and booster administrations to achieve and maintain efficacy. A multi-dose vaccination framework would need to account for partial protection after the first dose, adherence to the dosing schedule, waning immunity, and incomplete coverage. Including these features would likely reduce the overall impact of vaccination compared to the simplified assumptions used here and may shift the predicted conditions under which $R_e < 1$ can be achieved.

Despite these limitations, our approach provides a tractable framework for exploring how vaccination, in a generalized sense, interacts with relapse and treatment dynamics. A more detailed model incorporating age structure, dose-dependent vaccine efficacy, and operational constraints represents an important direction for future research and would support a more realistic evaluation of potential vaccination strategies for East Nusa Tenggara Province.

Data Availability

Available upon request.

Author Contributions

CWC and MZN were responsible for formulating and preparing the initial manuscript conceptualization. STY and JM assisted with modifying the model formulations. JM carried out a mathematical analysis. CWC and JM were involved in the numerical simulations assisted by SYT and their write-ups. All authors were involved in writing and approving the final manuscript version.

Appendix 1
The reproduction number of system (18)

Let $\boldsymbol{x_t} = (E_h, I_h, T_r, T_b, L_h, E_v, I_v)$. We define the vector $\mathcal{F}(\boldsymbol{x_t})$ whose ith entry represent the rate of new infections in the ith entry of the vector $\boldsymbol{x_t}$ and $\mathcal{V}(\boldsymbol{x_t})$ whose ith entry represent the transition rate out of the ith entry of the vector $\boldsymbol{x_t}$. Then, we can find

$$\mathcal{F}(\boldsymbol{x_t}) = \begin{pmatrix} \frac{bp_h(S_h+L_h)I_v}{N_h} \\ 0 \\ 0 \\ 0 \\ 0 \\ \frac{bp_m S_v(I_h+T_r+T_b)}{N_h} \\ 0 \end{pmatrix} \quad \mathcal{V}(\boldsymbol{x_t}) = \begin{pmatrix} \bar{a}_1 E_h \\ -\tau E_h - \psi L_h + \bar{a}_2 I_h \\ -(1-\varepsilon_t)\theta I_h + \bar{a}_3 T_r \\ -\varepsilon_t \theta I_h + \bar{a}_3 T_b \\ -(1-p)\gamma T_r + \frac{bp_h L_h I_v}{N_h} + \bar{a}_4 L_h \\ \bar{a}_5 E_v \\ -\kappa E_v + \mu_v I_v \end{pmatrix} \tag{20}$$

where $\bar{a}_1 = \mu_h + \tau$, $\bar{a}_2 = \mu_d + \mu_h + \theta$, $\bar{a}_3 = \gamma + \mu_h$, $\bar{a}_4 = \delta + \mu_h + \psi$, $\bar{a}_5 = \kappa + \mu_v$. We then find the matrix to represent the new infections and the transition between compartments by determining the Jacobian of $\mathcal{F}(\boldsymbol{x_t})$ and $\mathcal{V}(\boldsymbol{x_t})$ evaluated at the disease-free equilibrium $\mathcal{E}_1$. Let F and V be the respective Jacobian matrices of $\mathcal{F}(\boldsymbol{x_t})$ and

$\mathcal{V}(\boldsymbol{x_t})$ evaluated at the disease-free equilibrium,

$$F = \begin{pmatrix} 0 & 0 & 0 & 0 & 0 & 0 & bp_h \\ 0 & 0 & 0 & 0 & 0 & 0 & 0 \\ 0 & 0 & 0 & 0 & 0 & 0 & 0 \\ 0 & 0 & 0 & 0 & 0 & 0 & 0 \\ 0 & 0 & 0 & 0 & 0 & 0 & 0 \\ 0 & \frac{b\mu_h p_m \Lambda_v}{\Lambda_h \mu_v} & \frac{b\mu_h p_m \Lambda_v}{\Lambda_h \mu_v} & \frac{b\mu_h p_m \Lambda_v}{\Lambda_h \mu_v} & 0 & 0 & 0 \\ 0 & 0 & 0 & 0 & 0 & 0 & 0 \end{pmatrix}$$

and

$$V = \begin{pmatrix} \bar{a}_1 & 0 & 0 & 0 & 0 & 0 & 0 \\ -\tau & \bar{a}_2 & 0 & 0 & -\psi & 0 & 0 \\ 0 & -\theta(1-\epsilon_t) & \bar{a}_3 & 0 & 0 & 0 & 0 \\ 0 & -\theta\epsilon_t & 0 & \bar{a}_3 & 0 & 0 & 0 \\ 0 & 0 & -\gamma(1-p) & 0 & \bar{a}_4 & 0 & 0 \\ 0 & 0 & 0 & 0 & 0 & \bar{a}_5 & 0 \\ 0 & 0 & 0 & 0 & 0 & -\kappa & \mu_v \end{pmatrix}.$$

Appendix 2

Global Stability of DFE We show that the malaria-free equilibrium $\mathcal{E}_1$ is globally asymptotically stable (GAS) using the method described in [12]. First, we re-write system (18) as follows, let

$$\begin{cases} \dfrac{dX}{dt} &= F\big(X, \mathcal{I}\big), \\ \dfrac{d\mathcal{I}}{dt} &= \mathcal{G}\big(X, \mathcal{I}\big) \;\; \mathcal{G}\big(X, 0\big) = 0, \end{cases} \tag{21}$$

for $X = \big(S_h, S_v\big) \in \mathbb{R}^2$ and $\mathcal{I} = \big(E_h, I_h, T_r, T_b, L_h, E_v, I_v\big) \in \mathbb{R}^7$, where X and $\mathcal{I}$ represent the classes of the uninfectious and infectious individuals respectively. Next, we redefine the DFE as

$$\mathfrak{M}^* = (X_0, 0) = \big(S_h^*, E_h^*, I_h^*, T_r^*, T_b^*, L_h^*, S_v^*, E_v^*, I_v^*\big) = \left(\frac{\Lambda_h}{\mu_h}, 0, 0, 0, 0, 0, \frac{\Lambda_v}{\mu_v}, 0, 0\right).$$

According to [12], our malaria model given in (18) will be GAS at $\mathfrak{M}^*$ if the following conditions:

- $\mathfrak{C}_1$. $\mathfrak{M}^*$ is locally stable if $\mathcal{R}_0 < 1$,
- $\mathfrak{C}_2$. At $\dfrac{dX}{dt} = F(X_0, 0)$ the DFE is GAS,
- $\mathfrak{C}_3$. $\mathcal{G}(X, \mathcal{I}) = \mathcal{A}\mathcal{I} - \hat{\mathcal{G}}(X, \mathcal{I})$, $\hat{\mathcal{G}}(X, \mathcal{I}) \geq 0$ for $(X, \mathcal{I}) \in \Omega$, where $\mathcal{A} = \mathcal{D}_{\mathcal{I}}\mathcal{G}(X, \mathcal{I})$ is a Metzler matrix and Ω is the proposed model's feasible region,

are satisfied. Now, we establish that our model satisfies each of the above-enumerated conditions $\mathfrak{C}_1$ to $\mathfrak{C}_3$ to guarantee the GAS of the DFE. Clearly, since the model, basic reproduction number, $\mathcal{R}_0$, is calculated using the approach in Van den Driessche, and Watmough [37], it implies that $\mathfrak{M}^0$ is locally asymptotically stable whenever $\mathcal{R}_0 < 1$. Suppose $a_0 = (\mu_h + \tau)$, $a_1 = \Big(\mu_h + \theta\Big)$, $a_2 = (\mu_h + \gamma)$, $a_3 = (\psi + \delta)$, $a_4 = (\mu_v + \kappa)$, $\lambda_h = \dfrac{bp_h S_h I_v}{N_h}$, $\lambda_l = \dfrac{bp_h L_h I_v}{N_h}$ and $\lambda_v = \dfrac{bp_m S_v (I_h + T_r + T_b)}{N_h}$. Re-defining system (18) as to follow the form given in equation (18), we obtain

$$\frac{dX}{dt} = F(X, \mathcal{I}) = \begin{pmatrix} \Lambda_h - \lambda_h - \mu_h S_h + \delta L_h + \gamma T_b + p\gamma T_r \\ \Lambda_v - \lambda_l - \mu_v S_v \end{pmatrix},$$

$$\frac{d\mathcal{I}}{dt} = G(X,\mathcal{I}) = \begin{pmatrix} \lambda_h + \lambda_l - (\mu_h + \tau)E_h \\ \tau E_h + \psi L_h - (\theta + \mu_h)I_h \\ (1-\varepsilon_t)\theta I_h - (\mu_h + \gamma)T_r \\ \varepsilon_t \theta I_h - (\mu_h + \gamma)T_b \\ (1-p)\gamma T_r - \lambda_l - (\psi + \delta)L_h \\ \lambda_v - (\kappa + \mu_v)E_v \\ \kappa E_v - \mu_v I_v \end{pmatrix},$$

and

$$F(X,0) = \begin{pmatrix} \Lambda_h - \mu_h S_h \\ \Lambda_v - \mu_v S_v \end{pmatrix},$$

whose solutions yield a unique equilibrium point $\left(\frac{\Lambda_h}{\mu_h}, 0, 0, 0, 0, 0, \frac{\Lambda_v}{\mu_v}, 0, 0\right)$, thus being GAS, and therefore $\mathfrak{C}_2$ is satisfied. Linearizing the above second matrix gives a Metzler matrix as follows:

$$\mathcal{A} = \mathcal{D}_{\mathcal{I}}(\mathfrak{M}^*, 0) = \begin{pmatrix} -a_0 & 0 & 0 & 0 & 0 & 0 & \frac{bp_h S_h^0}{N_h^0} \\ \tau & -a_1 & 0 & 0 & \psi & 0 & 0 \\ 0 & (1-\varepsilon_t)\theta & -2 & 0 & 0 & 0 & \\ 0 & \varepsilon_t\theta & 0 & -a_2 & 0 & 0 & 0 \\ 0 & 0 & (1-p)\gamma & 0 & -a_3 & 0 & 0 \\ 0 & \frac{bp_m S_v^0}{N_h^0} & \frac{bp_m S_v^0}{N_h^0} & \frac{bp_m S_v^0}{N_h^0} & 0 & -a_4 & 0 \\ 0 & 0 & 0 & 0 & 0 & \kappa & -\mu_v \end{pmatrix}.$$

Solving for $\hat{\mathcal{G}}(X,\mathcal{I})$ and performing some algebraic manipulation yield

$$\hat{\mathcal{G}}(X,\mathcal{I}) = \mathcal{A}\mathcal{I} - \hat{\mathcal{G}}(X,\mathcal{I}) := \begin{pmatrix} bp_h\left[1 - \frac{N_h^0(S_v + L_h I_v)}{S_h^0 N_h}\right] \\ 0 \\ 0 \\ 0 \\ 0 \\ \frac{bp_m S_v}{N_h^0} \\ 0 \\ 0 \end{pmatrix}.$$

Setting $R_k = \frac{N_h^0(S_v + L_h I_v)}{S_h^0 N_h}$, we have the $0 \leq R_k \leq N_h$, and if $R_k < 0$, $\hat{\mathcal{G}}(X,\mathcal{I}) \geq 0$, then $\mathfrak{C}_3$ is satisfied as well. All the three conditions $\mathfrak{C}_1$ to $\mathfrak{C}_3$ are satisfied, and therefore, we can conclude that the DFE of the model system (18) is GAS whenever $\mathcal{R}_0 < 1$, which completes the proof.

Appendix 3

Endemic equilibrium for the model with two types of treatment

In this section, we determine the endemic equilibrium for system (18) denoted by $\mathcal{E}^\bullet = (S_h^\bullet, E_h^\bullet, I_h^\bullet, T_r^\bullet, T_b^\bullet, L_h^\bullet, S_v^\bullet, E_v^\bullet, I_v^\bullet)$. In order to obtain the endemic equilibrium $\mathcal{E}^\bullet$, we set the left-hand side

of system (18) to zero and solve the resulting system of equations. This system is given as follows:

$$\begin{cases} 0 &= \Lambda_h - p_h\lambda^\bullet S_h^\bullet I_v^\bullet - \mu_h S_h^\bullet + \delta L_h^\bullet + \gamma T_b^\bullet + p\gamma T_r^\bullet, \\ 0 &= p_h\lambda^\bullet (S_h^\bullet + L_h^\bullet) I_v^\bullet - \bar{a}_1 E_h^\bullet, \\ 0 &= \tau E_h^\bullet + \psi L_h^\bullet - \bar{a}_2 I_h^\bullet, \\ 0 &= (1-\varepsilon_t)\theta I_h^\bullet - \bar{a}_3 T_r^\bullet, \\ 0 &= \varepsilon_t \theta I_h^\bullet - \bar{a}_3 T_b^\bullet, \\ 0 &= (1-p)\gamma T_r^\bullet - p_h\lambda^\bullet L_h^\bullet I_v^\bullet - \bar{a}_4 L_h^\bullet, \\ 0 &= \Lambda_v - p_m\lambda^\bullet S_v^\bullet (I_h^\bullet + T_r^\bullet + T_b^\bullet) - \mu_v S_v^\bullet, \\ 0 &= p_m\lambda^\bullet S_v^\bullet (I_h^\bullet + T_r^\bullet + T_b^\bullet) - \bar{a}_5 E_v^\bullet, \\ 0 &= \kappa E_v^\bullet - \mu_v I_v^\bullet, \end{cases} \tag{22}$$

where $\bar{a}_1$, $\bar{a}_2$, $\bar{a}_3$, $\bar{a}_4$, $\bar{a}_5$ are defined as before and $\lambda^\bullet = b/N_h^\bullet$. For simplicity, the endemic equilibrium point $\mathcal{E}^\bullet$ will be expressed in terms of $\lambda^\bullet$. From the last equation of system (22) we obtain

$$E_v^\bullet = \frac{\mu_v I_v^\bullet}{\kappa}. \tag{23}$$

Adding the seventh and eighth equations of system (22) and solving for $S_v^\bullet$ gives

$$S_v^\bullet = \frac{\kappa\Lambda_v - \bar{a}_5\mu_v I_v^\bullet}{\kappa\mu_v}. \tag{24}$$

From the fourth and fifth equations of system (22) we have

$$T_r^\bullet = \frac{\theta I_h^\bullet (1-\varepsilon_t)}{\bar{a}_3} \qquad \text{and} \qquad T_b^\bullet = \frac{\theta I_h^\bullet \varepsilon_t}{\bar{a}_3}. \tag{25}$$

Substituting the expressions $T_r^\bullet$ and $T_b^\bullet$ given above into the eighth equation of system (22) and solving for $I_h^\bullet$ gives

$$I_h^\bullet = \frac{\bar{a}_3\bar{a}_5 I_v^\bullet \mu_v^2}{\lambda^\bullet (\bar{a}_3+\theta)\, p_m (\kappa\Lambda_v - \bar{a}_5 I_v^\bullet \mu_v)}. \tag{26}$$

Substituting the expression for $I_h^\bullet$ given in (26) into the expressions given in (25) gives

$$T_r^\bullet = \frac{\bar{a}_5\theta I_v^\bullet (1-\varepsilon_t)\,\mu_v^2}{\lambda^\bullet (\bar{a}_3+\theta)\, p_m (\kappa\Lambda_v - \bar{a}_5 I_v^\bullet \mu_v)} \qquad \text{and} \qquad T_b^\bullet = \frac{\bar{a}_5\theta I_v^\bullet \varepsilon_t \mu_v^2}{\lambda^\bullet (\bar{a}_3+\theta)\, p_m (\kappa\Lambda_v - \bar{a}_5 I_v^\bullet \mu_v)}. \tag{27}$$

Solving the sixth equation in (22) for $L_h^\bullet$ gives

$$L_h^\bullet = \frac{\bar{a}_5\gamma\theta(1-p) I_v^\bullet (1-\varepsilon_t)\,\mu_v^2}{\lambda^\bullet (\bar{a}_3+\theta)\, p_m (\bar{a}_4 + \lambda^\bullet p_h I_v^\bullet)(\kappa\Lambda_v - \bar{a}_5 I_v^\bullet \mu_v)}. \tag{28}$$

Substituting (26) and (28) into the third equation of (22) and solving for $E_h^\bullet$ gives

$$E_h^\bullet = \frac{\bar{a}_5 I_v^\bullet \mu_v^2 (\bar{a}_2\bar{a}_3 (\bar{a}_4 + \lambda^\bullet p_h I_v^\bullet) - \gamma\theta(1-p)\psi(1-\varepsilon_t))}{\lambda^\bullet\tau (\bar{a}_3+\theta)\, p_m (\bar{a}_4 + \lambda^\bullet p_h I_v^\bullet)(\kappa\Lambda_v - \bar{a}_5 I_v^\bullet \mu_v)}. \tag{29}$$

Substituting (28) and (29) into the second equation of (22) and solving for $S_h^\bullet$ gives

$$S_h^\bullet = \frac{\bar{a}_5\mu_v^2\left(\bar{a}_1\left(\gamma\theta(1-p)\psi\left(1-\varepsilon_t\right)-\bar{a}_2\bar{a}_3\left(\bar{a}_4+\lambda^\bullet p_h I_v^\bullet\right)\right)+\gamma\theta\lambda^\bullet(p-1)\tau p_h I_v^\bullet\left(\varepsilon_t-1\right)\right)}{\lambda^{\bullet^2}\tau\left(\bar{a}_3+\theta\right)p_h p_m\left(\bar{a}_4+\lambda^\bullet p_h I_v^\bullet\right)\left(\bar{a}_5 I_v^\bullet\mu_v-\kappa\Lambda_v\right)}. \tag{30}$$

Notice that equations (23) - (30) are expressed in terms of $I_v^\bullet$. Thus, substituting equations (23) - (30) into the first equation of system (22) leads to the following second-order polynomial equation in terms of $I_v^\bullet$,

$$\chi_2\left(I_v^\bullet\right)^2+\chi_1 I_v^\bullet+\chi_0=0, \tag{31}$$

where

$$\begin{aligned}
\chi_0 &= \bar{a}_1\bar{a}_2\bar{a}_3\bar{a}_4\bar{a}_5\mu_h\mu_v^2(1-\Phi_t)\left(1-\mathcal{R}_e^t\right),\\
\chi_1 &= \lambda^\bullet p_h(\bar{a}_5\mu_v(\bar{a}_4\lambda^\bullet\tau(\bar{a}_3+\theta)\Lambda_h p_m+\mu_v(\gamma\theta\tau(\bar{a}_4((p-1)\varepsilon_t-p)-(1-p)(1-\epsilon_t)(\delta+\mu_h))\\
&\quad +\bar{a}_1(\bar{a}_2\bar{a}_3(\bar{a}_4+\mu_h)-\gamma\theta(1-p)\psi(1-\varepsilon_t))))-\kappa\lambda^{\bullet^2}\tau(\bar{a}_3+\theta)\Lambda_h p_h p_m\Lambda_v),\\
\chi_2 &= \bar{a}_5\lambda^{\bullet^2}p_h^2\mu_v\left(\mu_v\left(\bar{a}_1\bar{a}_3\mu_d+\mu_h\left(\mu_h\left(\bar{a}_1+\gamma+\theta\right)+\tau(\gamma+\theta)+\gamma\theta\right)\right)+\lambda^\bullet\tau\Lambda_h p_m\left(\gamma+\mu_h+\theta\right)\right),
\end{aligned} \tag{32}$$

with

$$\mathcal{R}_e^t=\left[\left(\frac{\lambda^\bullet\Lambda_h}{b\mu_h}\right)\mathcal{R}_0^t\right]^2. \tag{33}$$

We note from (32) that

$$\chi_0>0 \quad \text{when} \quad \mathcal{R}_e^t<1 \quad \text{or} \quad \chi_0<0 \quad \text{when} \quad \mathcal{R}_e^t>1.$$

Also, note that there is a possibility that either $\chi_1>0$ or $\chi_1<0$. Lastly, it can be clearly noted that $\chi_2>0$. Thus, we have the following results on the existence of $\mathcal{E}^\bullet$ for system (18).

REFERENCES

1. CentralbureauofstatisticsIndonesia,UmurHarapanHidupSaatLahir(UHH)(Tahun),20192020. Accessed: 2024-03-12.
2. About Malaria, Biology. https://www.cdc.gov/malaria/about/biology/index.html. Accessed: 2024-05-12.
3. Frequently Asked Questions (FAQs), https://www.who.int/news-room/fact-sheets/detail/malaria@misc{FAQ,}. Accessed: 2022-09-12.
4. Frequently Asked Questions (FAQs), https://www.cdc.gov/malaria/about/faqs.html. Accessed: 2022-09-12.
5. Malaria Elimination and Eradication, https://www.ncbi.nlm.nih.gov/books/NBK525190/. Accessed: 2023-01-12.
6. Malaria (Key facts), https://www.who.int/news-room/fact-sheets/detail/malaria@misc{Keyfacts,} Accessed: 2023-01-02.
7. Radical cure for Plasmodium vivax malaria, https://www.vivaxmalaria.org/diagnosis-treatment/treatment/radical-cure-for-plasmodium-vivax-malaria$#$:œ:text=Radical$%$20cure$$20requires$%$20the$%$0administration,ACT)$%$20to$%$0clear$%$20blood$%$20stages. Accessed: 2024-05-14.
8. Indonesia Health Ministry Jakarta, Indonesia's Health Profile 2018 https://pusdatin.kemkes.go.id/resources/download/pusdatin/profil-kesehatan-indonesia/PROFIL_KESEHATAN_2018_1.pdf. Accessed: 2024-03-12.
9. F. B. Agusto, S. Y. Del Valle, K. W. Blayneh, C. N. Ngonghala, M. J. Goncalves, N. Li, R. Zhao, and H. Gong, *The impact of bed-net use on malaria prevalence*, Journal of Theoretical Biology, vol. 320, pp. 58–65, 2013.
10. D. Aldila, *Dynamical analysis on a malaria model with relapse preventive treatment and saturated fumigation*, Computational and Mathematical Methods in Medicine, vol. 2022, 2022.
11. S. M. Blower and H. Dowlatabadi, *Sensitivity and uncertainty analysis of complex models of disease transmission: an HIV model, as an example*, International Statistical Review, pp. 229–243, 1994.
12. C. Castillo Chavez, Z. Feng, and W. Huang, *On the computation of R_0 and its role on global stability*, Mathematical Approaches for Emerging and Re-emerging Infection Diseases, vol. 125, pp. 31–65, 2002.
13. G. Chowell, *Fitting dynamic models to epidemic outbreaks with quantified uncertainty*, Infectious Disease Modelling, vol. 2, no. 3, pp. 379–398, 2017.

14. C. W. Chukwu, M. L. Juga, Z. Chazuka, and J. Mushanyu, *Mathematical analysis and sensitivity assessment of HIV/AIDS–listeriosis co-infection dynamics*, International Journal of Applied and Computational Mathematics, vol. 8, no. 5, p. 251, 2022.
15. C. W. Chukwu, J. Mushanyu, M. L. Juga, and Z. Chazuka, *A mathematical model for co-dynamics of listeriosis and bacterial meningitis diseases*, Commun. Math. Biol. Neurosci., Article–ID, 2020.
16. T. S. Detinova, D. S. Bertram, and World Health Organization, *Age-grouping methods in Diptera of medical importance*, World Health Organization, 1962.
17. S. Dhiman, *Are malaria elimination efforts on right track?*, Infectious Diseases of Poverty, vol. 8, no. 1, pp. 1–19, 2019.
18. Health Department of ENTP, Kupang NTT Indonesia: 2019. Health Profile of East Nusa Tenggara Province (ENTP) 2018 https://dinkes.nttprov.go.id/index.php/publikasi/publikasi-data-dan-informasi., Accessed: 2024-03-12.
19. Centers for Disease Control and Prevention, Malaria https://www.cdc.gov/malaria/glossary.html$#$:œ:text=Radical$%$20cure$%3A%$20(also$%3%$20radical,ovale., Accessed: 2024-05-16.
20. S. Gao, P. Binod, C. W. Chukwu, T. Kwofie, S. Safdar, L. Newman, S. Choe, B. K. Datta, W. K. Attipoe, and W. Zhang, *A mathematical model to assess the impact of testing and isolation compliance on COVID-19*, Infectious Disease Modelling, vol. 8, no. 2, pp. 427–444, 2023.
21. M. Ghosh, S. Olaniyi, and O. S. Obabiyi, *Mathematical analysis of reinfection and relapse in malaria dynamics*, Applied Mathematics and Computation, vol. 373, p. 125044, 2020.
22. R. D. Guntur, J. Kingsley, and F. M. A. Islam, *Epidemiology of malaria in East Nusa Tenggara Province*, JMIR Research Protocols, vol. 10, no. 4, e23545, 2021.
23. B. D. Handari, R. A. Ramadhani, C. W. Chukwu, S. H. A. Khoshnaw, and D. Aldila, *An optimal control model to understand the potential impact of the new vaccine*, Vaccines, vol. 10, no. 8, p. 1174, 2022.
24. F. F. Herdicho, W. Chukwu, H. Tasman, and P. A. Dumbela, *An optimal control of malaria transmission model with mosquito seasonal factor*, Results in Physics, vol. 25, p. 104238, 2021.
25. S. Z. John, H. U. Yusuf, S. A. Usman, and S. Adamu, *Mathematical model for the dynamics of malaria transmission*, Science Forum, vol. 20, pp. 124–124, 2020.
26. C. E. Madubueze, Z. Chazuka, I. O. Onwubuya, F. Fatmawati, and C. W. Chukwu, *On the mathematical modeling of schistosomiasis transmission dynamics with heterogeneous intermediate host*, Frontiers in Applied Mathematics and Statistics, vol. 8, p. 1020161, 2022.
27. M. Z. Ndii and Y. A. Adi, *Understanding the effects of individual awareness and vector controls on malaria transmission dynamics using multiple optimal control*, Chaos, Solitons and Fractals, vol. 153, p. 111476, 2021.
28. K. O. Okosun, R. Ouifki, and N. Marcus, *Optimal control analysis of a malaria disease transmission model that includes treatment and vaccination with waning immunity*, Biosystems, vol. 106, no. 2–3, pp. 136–145, 2011.
29. World Health Organization, *World malaria report 2014: summary*, World Health Organization, 2015.
30. K. P. Paaijmans and M. B. Thomas, *The influence of mosquito resting behaviour and associated microclimate for malaria risk*, Malaria Journal, vol. 10, pp. 1–7, 2011.
31. R. N. Price, L. Von Seidlein, N. Valecha, F. Nosten, J. K. Baird, and N. J. White, *Global extent of chloroquine-resistant Plasmodium vivax: a systematic review and meta-analysis*, The Lancet Infectious Diseases, vol. 14, no. 10, pp. 982–991, 2014.
32. M. Roy, M. J. Bouma, E. L. Ionides, R. C. Dhiman, and M. Pascual, *The potential elimination of Plasmodium vivax malaria by relapse treatment: insights from a transmission model and surveillance data from NW India*, PLoS Neglected Tropical Diseases, vol. 7, no. 1, e1979, 2013.
33. M. E. Sinka, M. J. Bangs, S. Manguin, T. Chareonviriyaphap, A. P. Patil, W. H. Temperley, P. W. Gething, I. R. F. Elyazar, C. W. Kabaria, and R. E. Harbach, *The dominant Anopheles vectors of human malaria in the Asia-Pacific region: occurrence data, distribution maps and bionomic précis*, Parasites & Vectors, vol. 4, pp. 1–46, 2011.
34. H. Tasman, U. D. Purwati, F. F. Herdicho, and C. W. Chukwu, *An optimal control problem of malaria model with seasonality effect using real data*, Commun. Math. Biol. Neurosci., Article–ID, 2021.
35. H. Tasman, D. Aldila, P. A. Dumbela, M. Z. Ndii, F. F. Herdicho, C. W. Chukwu, and Fatmawati, *Assessing the impact of relapse, reinfection and recrudescence on malaria eradication policy: a bifurcation and optimal control analysis*, Tropical Medicine and Infectious Disease, vol. 7, no. 10, p. 263, 2022.
36. S. Y. Tchoumi, C. W. Chukwu, M. L. Diagne, H. Rwezaura, M. L. Juga, and J. M. Tchuenche, *Optimal control of a two-group malaria transmission model with vaccination*, Network Modeling Analysis in Health Informatics and Bioinformatics, vol. 12, no. 1, p. 7, 2022.
37. P. Van den Driessche and J. Watmough, *Reproduction numbers and sub-threshold endemic equilibria for compartmental models of disease transmission*, Mathematical Biosciences, vol. 180, no. 1–2, pp. 29–48, 2002.
38. K. Vogt-Geisse, C. N. Ngonghala, and Z. Feng, *The impact of vaccination on malaria prevalence: a vaccine-age-structured modeling approach*, Journal of Biological Systems, vol. 28, no. 2, pp. 475–513, 2020.
39. Fatmawati, H. Tasman, F. F. Herdicho, and others, *An optimal control problem of malaria model with seasonality effect using real data*, Communications in Mathematical Biology and Neuroscience, 2021.
40. R. D. Guntur, J. Kingsley, and F. M. A. Islam, *Malaria awareness of adults in high, moderate and low transmission settings: A cross-sectional study in rural East Nusa Tenggara Province, Indonesia*, PLoS ONE, 2021.
41. M. Lobo, R. D. Guntur, and others, *The declined trend of malaria over a ten-year period in rural East Nusa Tenggara Province, Indonesia: A medical record analysis*, Open Access Macedonian Journal of Medical Sciences, 2024.
42. R. D. Guntur, J. Pahnael, and others, *Modeling malaria risk factors by logistic regression among hilly communities in rural East Nusa Tenggara Province, Indonesia*, Mathematical Modeling and Engineering Problems, 2025.